PHYSICAL REVIEW B **86**, 161201(R) (2012)

Spatially resolved photocarrier energy relaxation in low-doped bulk GaAs

T. Kiessling,* J.-H. Quast, A. Kreisel, T. Henn, W. Ossau, and L. W. Molenkamp
Physikalisches Institut (EP3) der Universität Würzburg, 97074 Würzburg, Germany
(Received 18 July 2011; revised manuscript received 13 April 2012; published 22 October 2012)

We report on spatially resolved cw-photoluminescence studies of very-low-doped *n*- and *p*-type GaAs, which demonstrate that optically excited electrons retain significant excess energy on length scales of several tens of microns away from the excitation point. In contrast, the lattice is heated only negligibly outside the optical excitation area even for moderate excitation intensities. When diffusing away from the excitation site the photoelectrons are therefore not in thermal equilibrium with the lattice. Our results imply that it is inappropriate to describe low temperature photocarrier diffusion in GaAs with a spatially uniform diffusion constant.

DOI: 10.1103/PhysRevB.86.161201 PACS number(s): 78.20.−e, 72.25.Dc, 78.55.Cr

Investigations on spin drift and diffusion lengths in GaAs have shown that a nonequilibrium spin distribution (NESD) can propagate over spatial distances on the order of 100 μm,[1–5] which is an important step towards proving the feasibility of spintronic architectures. For these studies, the NESD was either invoked electrically, through ferromagnetic contacts,[5,6] or optically, by circularly polarized light in a magneto-optical Kerr effect (MOKE) pump-probe configuration.[2–4] In all of those experiments the electron system gains considerable excess energy with respect to the lattice.

The extraction of characteristic spin propagation parameters in the above investigations is commonly done on the basis of simple diffusion models.[4] Early experiments already reported spin diffusion values in excess of what was expected from carrier mobilities,[7] thus violating the Einstein relation. For degenerate semiconductors, this discrepancy was soon resolved theoretically within the frame of drift-diffusion models.[8] However, recent experiments on spin propagation in nondegenerate semiconductors also indicate spin diffusion constants that significantly exceed the corresponding charge diffusion parameters obtained from the carrier mobilities.[4] Existing models that take Coulomb correlations into account predict the opposite trend, i.e., the spin diffusion constant should be reduced with respect to carrier diffusion constant due to Coulomb drag.[9,10]

The modeling in most previous studies employs a spatially uniform diffusion constant. This is justified if no thermal gradients exist in the spin system, which implies that the NESD is in thermal equilibrium with the lattice system. Experimentally, enhanced spin relaxation times are often reported on a relatively low-doped material, where Dyakonov-Perel relaxation is suppressed. On the other hand, for low carrier concentrations it is well established that at low lattice temperatures photoelectrons are not in thermal equilibrium with the lattice at the point of their excitation.[11,12] If this situation persists outside the pumped area and on length scales comparable to the determined spin diffusion lengths, a spatially uniform diffusion constant is inappropriate for the description of spatial spin propagation.

In order to provide insight into the spatial dependence of the excess energy of the electron and lattice systems we have performed a systematic investigation on very-low-doped *n*- and *p*-type GaAs. Photoluminescence (PL) studies on very pure GaAs offer the unique possibility of extracting the temperature of both the electron and lattice system independently. By measuring spatially resolved PL, one can therefore extract possible differences in the characteristic length scales for heat relaxation.

The experiments have been performed on two (100) oriented liquid phase epitaxy grown GaAs layers with a thickness of 70 μm, unintentionally doped to 3×10^{13} cm^{-3} (p) and 2×10^{13} cm^{-3} (n) at room temperature, respectively. PL is excited by a diode pumped solid state laser at $\lambda = 785$ nm and detected by a Si avalanche photodiode mounted on a 1 m focal length spectrometer equipped with a 1200 mm^{-1} grating. The samples are kept in a bath cryostat, in which they are immersed in liquid He for temperatures below 4.2 K and in He exchange gas for temperatures above. For the spatially resolved experiments the excitation is focused to a $\omega_L = 8.0$ μm ($\frac{1}{e}$) spot diameter by an infinity corrected microscope objective, through which the PL signal is collected in confocal geometry. For spatial pickup, the PL is focused by a plano-convex lens, which is mounted on a three-dimensional (3D) micrometer translation stage, onto an intermediate 30 μm pinhole. Moving the position of the lens allows to spatially filter the PL signal in front of the entrance slit of the spectrometer. With the lenses employed, the setup yields a spatial optical resolution of 10 μm.

Typical nonspatially resolved PL spectra of the samples are displayed in Fig. 1. To gauge the lattice temperature we use the excitons bound to neutral acceptors that are evident in the spectra, while the temperature of the electron system can be probed by analyzing the electron-acceptor transition.

Lattice temperature. The results obtained for the two samples agree within error bars, so we limit ourselves to showing data on the *p*-type sample, which enables extraction of more robust values due to the enhanced PL spectral weight of the acceptor bound states. As a result of the *j*-*j* coupling of the acceptor bound hole and the exciton, this transition yields three characteristic lines upon radiative recombination, indicated by (A^0,X) in Figs. 1(b) and 1(d).[13] Their relative intensities display a pronounced temperature dependence that stems from the thermal distribution of the excitons. Because this transition occurs from a bound state, only excitons that relax their excess kinetic energy may contribute, and the thermal occupation of the fine structure is consequently given exclusively by the lattice temperature. The relative intensities of the (A^0,X) transition are therefore a very sensitive probe of the latter.

Extraction of absolute temperatures from the PL spectra is, however, complicated by both theoretical and experimental limitations. On the theoretical end, the degeneracies and

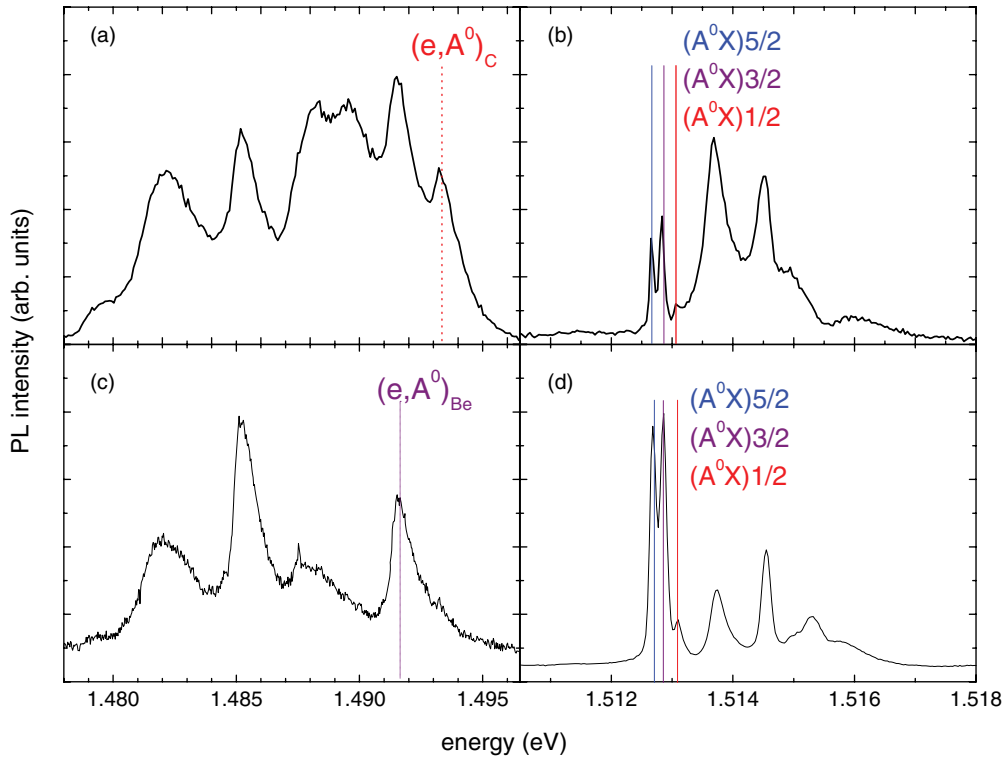

FIG. 1. (Color) Photoluminescence spectra of low-doped n-type [(a),(b)] and p-type [(c),(d)] 70 μm thick GaAs layers. Displayed are the excitonic [(b),(d)] and impurity [(a),(c)] spectral regions of both samples. Indicated are the electron neutral acceptor transitions (eA^0) on which the electron temperature and the neutral acceptor bound exciton transitions (A^0,X) on which the lattice temperature were extracted, respectively.

oscillator strengths of the individual (A^0,X) lines are not unambiguously known. Early theoretical work taking into account only short range exchange interactions suggested a spectral weighting of the 5/2, 3/2, and 1/2 lines as 1:4:1.[14] Already then it was realized that the energy splittings emerging from the calculations fall short from the experiments by at least one order of magnitude. Likewise, the proposed sequence fails to account for the temperature evolution of the intensities. Theoretical work taking into account long range exchange contributions and/or excited excitonic states is lacking. On the experimental side, the extraction of the (A^0,X) line intensity is complicated by the presence of spectrally nearby excitonic transitions such as the (D^+,X) line at 1.5137 eV (see Fig. 1), which themselves are subject to change with increasing temperature. Rather than trying to establish absolute temperatures, we therefore choose to measure the relative intensities of the $(A^0,X)_{5/2}$ to $(A^0,X)_{3/2}$ transition as a function of temperature, and use this information to characterize the spatial dependence of the lattice temperature.

We first note that lattice heating critically depends on the excitation intensity. To compare with MOKE studies the intensity is set to 1×10^4 W/cm^{-2}, which resembles typical probe intensities (pump intensities are typically several orders of magnitude lower). For this excitation density the relative intensities of the $(A^0,X)_{5/2}$ to the $(A^0,X)_{3/2}$ transition were measured as function of bath temperature in the regime from 1.6 to 2.1 K. The results are displayed in Fig. 2(a). Clearly, the (A^0,X) transition is capable of resolving temperature changes as small as 0.2 K in this temperature region. It is, however, incorrect to infer absolute lattice temperatures from these data, as can be seen from the spatial dependence of the (A^0,X) signal. In Fig. 2(b), the relative intensities of the $(A^0,X)_{5/2}$ to the $(A^0,X)_{3/2}$ transition were detected as a function of position on the sample relative to the excitation spot at the lowest temperature of 1.6 K used here.

For these excitation conditions, the lower energetic $(A^0,X)_{5/2}$ line gains spectral weight at distances up to 30 μm away from the excitation spot, at which point the intensity ratio becomes constant. This observation obviously indicates that the lattice temperature in the laser spot is always elevated with respect to the heat bath. Repeating this experiment for increased bath temperatures yields that this optically induced thermal gradient is reduced with increasing bath temperature and vanishes for $T > 8$ K [see the inset of Fig. 2(b)]. This result is consistent with expectation, as the thermal conductivity of the lattice increases with increasing phonon occupation at elevated temperatures.[15]

Summarizing, the above results yield the following picture: Lattice heating is only relevant for high intensities and at very low temperatures. The excess heat relaxes on a length scale of 30 μm and becomes insignificant as the bath temperature is increased. Comparing intensity ratios for the $(A^0,X)_{5/2}$ and $(A^0,X)_{3/2}$ transition away from the excitation spot, one can extract an upper boundary for the absolute value of the lattice temperature in the spot. We find a lattice temperature of $\approx$6 K in the laser spot at a bath temperature of $T = 1.6$ K.

Electron temperature. The radiative recombination of a conduction band electron to a neutral acceptor (e,A^0) is a

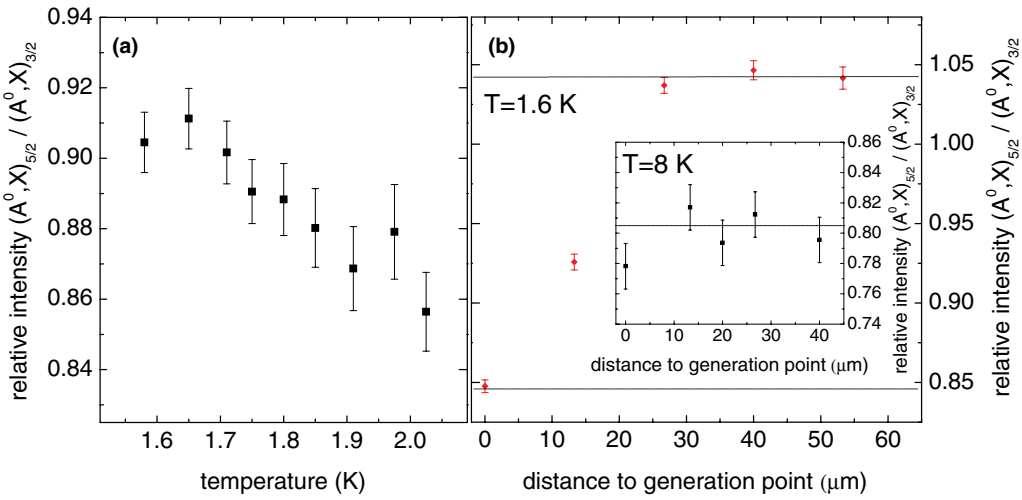

FIG. 2. (Color) Lattice temperature extracted from neutral acceptor bound exciton transitions of the p-type GaAs layer. (a) Relative intensities of the $(A^0,X)_{5/2}$ to the $(A^0,X)_{3/2}$ transition as function of bath temperature for high intensity (10^4 W/cm^{-2}) excitation. (b) Spatial dependence of the relative intensities of the $(A^0,X)_{5/2}$ to the $(A^0,X)_{3/2}$ transition at a bath temperature of $T = 1.6$ K. Inset: Same for a bath temperature of $T = 8$ K.

transition from an energetically continuous initial state to an energetically discrete final state. The line shape of the (e,A^0) transition is therefore solely given by the thermal distribution of the electrons in the conduction band and its intensity as a function of PL energy E is described by[16]

$$I(E) \propto \sqrt{E - E_A}\exp\left[-\frac{E - E_A}{k_B T_e}\right], \tag{1}$$

where $E_A = E_\Gamma - E_{A0}$, with E_Γ the fundamental band gap and E_{A0} the neutral acceptor binding energy at the Γ point, k_B is the Boltzmann constant, and T_e the electron temperature.

Fitting Eq. (1) to the high energy side of the (e,A^0) transition, one can accurately extract the temperature of the electron system as long as no energetically nearby transitions disturb the line shape. This requirement is well met for the carbon (n) and beryllium (p) acceptor transitions in our samples (see Fig. 1) and we have used these transitions to establish the electron temperature relative to the lattice temperature. To avoid lattice heating, low excitation intensities of $I = 10$ W/cm^{-2} were employed. Under these conditions no spatial change of the intensity ratios of the (A^0,X) transitions was observed. These are, moreover, typical values for pump power densities in spatially resolved MOKE experiments.[3,4]

We first note that these line fits agree very well with the data [see the inset of Fig. 3(b)], which means that the electrons are described by a Maxwellian distribution. This indicates that photoelectrons and intrinsic electrons have thermalized upon recombination, i.e., the electron system itself is in thermal equilibrium. The resulting electron temperature as a function of the lattice temperature for the above excitation conditions is displayed in Fig. 3(a). The plot confirms that irrespective of the doping type, up to lattice temperatures of 25 K the electron temperature sizably exceeds the lattice temperature. These findings agree well with established literature, where it is understood that this excess energy is a direct consequence of the small thermal coupling of the electron and lattice systems at low temperatures, where longitudinal optic (LO) phonon states are energetically inaccessible.[12,15] Previous investigations also showed that the excess energy in the electron system critically depends on excitation intensity. It saturates in GaAs for low temperatures at pump fluences which are three orders of magnitude lower than the ones used in our experiments, without ever reaching a regime at which the excess heat goes to zero.[11] We can thus deduce that our findings will also be relevant at significantly higher doping concentrations. They are also consistent with time domain investigations, which find several meV of average excess energy for photocarriers with respect to the lattice temperature. In the low doping regime of our samples the electrons retain significant excess energy even after 10 ns, which is the typical order of magnitude of the radiative lifetime.[11]

The question then arises, over which spatial distances this nonequilibrium situation persists. The spatial dependence of the electron temperature was determined for a lattice temperature of $T = 8$ K and is shown in Fig. 3(b). In both n- and p-type GaAs, the electrons display excess heat on a length scale of several tens of microns.

We model the steady state electron temperature profile by the heat equation

$$\nabla[K(u)\nabla u(r,z)] + a(u) = g, \tag{2}$$

where $u(r,z)$ is the electron temperature in cylindrical coordinates. For a TEM$_{00}$ excitation spot with a $\frac{1}{e}$ width ω_g and an absorption depth z_g, the generation term g takes the form

$$g = g_0\left(\pi\omega_g^2 z_g\right)^{-1}\exp\left[-\left(\frac{r}{\omega_g}\right)^2 - \left(\frac{z}{z_g}\right)\right]. \tag{3}$$

Here, $g_0 = \frac{(1-R)P_{\text{laser}}}{E_{\text{ph}}}E_e$ with P_{laser} and E_{ph} designating the excitation power and photon energy, respectively, and R is the sample reflectance. The excess energy per excited electron is given by

$$E_e = (E_{\text{ph}} - E_{\text{gap}})\left(1 + \frac{m_e}{m_h}\right)^{-1} - i\hbar\omega_{\text{LO}}, \quad i \text{ integer}, \tag{4}$$

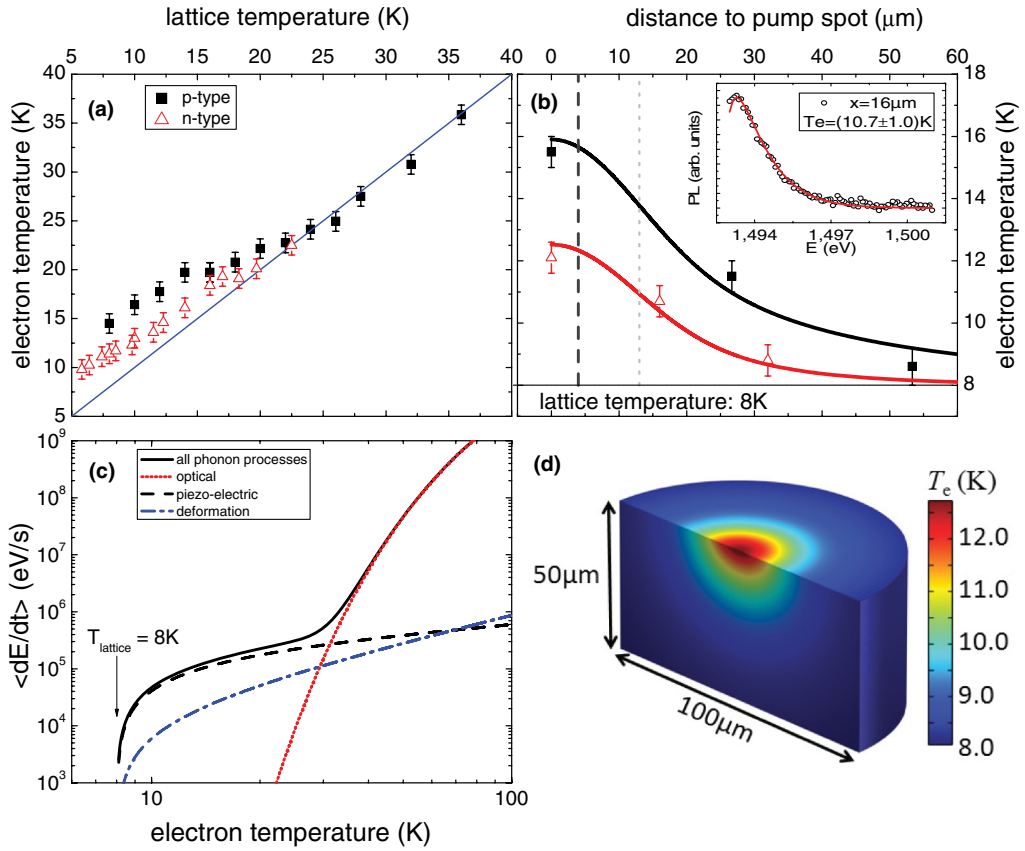

FIG. 3. (Color) Electron temperature extracted from the electron neutral acceptor transition. (a) Electron temperature vs lattice temperature for low intensity excitation (10 W/cm^{-2}). (b) Spatial dependence of the electron temperature measured (symbols) and calculated (line) at a lattice temperature of $T = 8$ K. The dashed (dotted) line indicates the laser spot size ω_L (photocarrier diffusion length ω_n). Inset: Exemplary fit to PL data for extraction of T_e according to Eq. (1). (c) Average energy loss rate per electron for Maxwell-Boltzmann distributed electrons (Ref. 11). (d) Calculated electron temperature profile for n-GaAs (Ref. 17).

where E_{gap} is the fundamental band gap, $m_{e,(h)}$ the electron (hole) band mass, and $\hbar\omega_{\text{LO}}$ the energy of LO(Γ) phonons. The last term accounts for fast optical phonon scattering which occurs when E_e exceeds $\hbar\omega_{\text{LO}}$. The model therefore does not account for very fast processes, which are relevant before there is a temperature established. However, photocarriers outdiffuse even before thermalizing. For steady state modeling this means that the relevant quantity for the lateral length scale of the generation term in Eq. (3) is the photocarrier diffusion length ω_n, for which ω_g has to be replaced. The energy dissipation term can be written as

$$a(u) = n(r,z)\left(\left\langle\frac{dE}{dt}\right\rangle_{\text{op}} + \left\langle\frac{dE}{dt}\right\rangle_{\text{pe}} + \left\langle\frac{dE}{dt}\right\rangle_{\text{ac}}\right). \qquad (5)$$

This expression, due to Ulbrich,[11] takes into account the averaged energy loss rates $\langle dE/dt\rangle$ per electron for polar-optical (op), piezoelectric (pe), and acoustic deformation potential (ac) scattering in a Maxwellian distribution of electrons with temperature T_e. As an example, Fig. 3(c) plots the loss rates calculated for a lattice temperature of $T = 8$ K. The electron density is given by

$$n(r,z) = \frac{2(1-R)\tau P_{\text{laser}}}{E_{\text{ph}}\left(\pi^{3/2}\omega_n^3\right)} \exp\left[-\frac{r^2+z^2}{\omega_n^2}\right] + n_{\text{int}}, \qquad (6)$$

where n_{int} denotes the intrinsic electron density. The first term describes the spatial distribution of photoelectrons, with τ being the radiative lifetime and ω_n the photoelectron diffusion length. Low temperature heat conduction of low-doped GaAs is almost entirely due to phonons and data on the contribution of electrons are needed. We approximate the thermal diffusivity $K(u)$ of electrons as that of an ideal gas:

$$K(u) = \frac{\langle v\rangle l c_e n(r,z)}{3}, \quad \text{with} \quad \langle v\rangle = \sqrt{\frac{3k_B T_e}{m_e}}. \qquad (7)$$

The mean free path between e-e scattering events $l = [\sigma\, n(r,z)]^{-1}$ is assumed to be given by the wavelength of the quasiparticle $\lambda_e = h/\sqrt{2\pi m_e k_B T_e}$ through $\sigma = \pi\lambda_e^2$, whereas the heat capacity per electron $c_e = \frac{3}{2}k_B$.

Employing the finite-element method we solve Eq. (2) numerically, the result of which is displayed in Fig. 3(d). While there are no actual free parameters, we do not have direct experimental access to ω_n, which thus was adjusted for optimal agreement with the data under the condition $\omega_n \geqslant \omega_g$. The model succeeds in quantitatively describing the experimental findings. This clearly means that one cannot assume that the electrons are in thermal equilibrium with the lattice outside the pump area and just take their temperature to be that of the

heat bath. The equilibration length scale is very comparable to typical spin diffusion lengths reported in low-doped GaAs.[3]

Conclusions. We have demonstrated that under the typical experimental conditions of optical pump-probe experiments at low lattice temperatures both the electron and the lattice may gain sizable excess heat, which is sustained on length scales of several tens of microns. While heating of the lattice can be avoided by using low optical power density, electron heating results from the excess energy of photocarriers induced by the optical pumping process and is therefore a feature of all low temperature (<25 K) experiments with above band-gap excitation conditions.

The electron temperature can be significantly higher than the lattice temperature, easily exceeding the latter by more than a factor of 3. Its magnitude is set by the excess energy of photogenerated electrons. At low lattice temperature, the increased electron temperature in the excitation spot will inevitably result in the buildup of a thermal gradient in the electron system, on a scale of tens of microns where energy relaxation by optical phonons is ineffective. This result is also relevant for architectures in which the electrons are injected electrically, especially through tunnel barriers. While the injected to intrinsic carrier ratio may compare favorably to typical optical experiments as a result of higher doping concentrations, the excess energy of electrically injected electrons can easily be 100 meV and above.[18] Concerning spin diffusion experiments in GaAs, this may explain some of the apparent discrepancies between carrier mobilities, which are robustly measured by transport experiments, and the observed spin drift and diffusion lengths.

The authors thank G. V. Astakhov for fruitful discussion. Financial support by the DFG (OS98/9-2) is gratefully acknowledged.

*tobias.kiessling@physik.uni-wuerzburg.de

[1] R. Dzhioev, B. Zakharchenya, V. Korenev, and M. Stepanova, Phys. Solid State **39**, 1765 (1997).

[2] J. Stephens, J. Berezovsky, J. P. McGuire, L. J. Sham, A. C. Gossard, and D. D. Awschalom, Phys. Rev. Lett. **93**, 097602 (2004).

[3] S. A. Crooker and D. L. Smith, Phys. Rev. Lett. **94**, 236601 (2005).

[4] M. Furis, D. L. Smith, S. Kos, E. S. Garlid, K. S. M. Reddy, C. J. Palmstrøm, P. A. Crowell, and S. A. Crooker, New J. Phys. **9**, 347 (2007).

[5] S. A. Crooker, M. Furis, X. Lou, C. Adelmann, D. L. Smith, C. J. Palmstrøm, and P. A. Crowell, Science **309**, 2191 (2005).

[6] C. Adelmann, X. Lou, J. Strand, C. J. Palmstrøm, and P. A. Crowell, Phys. Rev. B **71**, 121301(R) (2005).

[7] J. M. Kikkawa and D. D. Awschalom, Nature (London) **397**, 139 (1999).

[8] M. E. Flatté and J. M. Byers, Phys. Rev. Lett. **84**, 4220 (2000).

[9] I. D'Amico and G. Vignale, Phys. Rev. B **62**, 4853 (2000).

[10] I. D'Amico and G. Vignale, Europhys. Lett. **55**, 566 (2001).

[11] R. Ulbrich, Phys. Rev. B **8**, 5719 (1973).

[12] H. Münzel, A. Steckenborn, and D. Bimberg, J. Lumin. **24/25**, 569 (1981).

[13] A. M. White, P. J. Dean, and B. Day, J. Phys. C **7**, 1400 (1974).

[14] B. Stébé and G. Munschy, Solid State Commun. **40**, 663 (1981).

[15] M. G. Holland, *Semiconductors and Semimetals*, edited by R. K. Willardson and A. C. Beer, Vol. 2 (Academic, New York, 1966), p. 3.

[16] D. M. Eagles, J. Phys. Chem. Solids **16**, 76 (1960).

[17] For modeling the following values were used: general: $\omega_n = 13\ \mu$m, $z_g = 0.7\ \mu$m, $E_{\rm ph} = 1.579$ eV, $E_{\rm gap} = 1.519$ eV, $m_e = 0.067m_0$, $m_h = 0.51m_0$, $\hbar\omega_{\rm LO} = 36$ meV, $R = 0.3$, $\tau = 7$ ns; for scattering rates (Ref. 11): $\varepsilon_\infty = 10.9$, $\varepsilon_0 = 12.5$, $e_{14} = 0.16\ {\rm C/m^2}$, $a = 0.4$, $E_1 = 6.3$ eV, $\rho = 5316\ {\rm kg/m^3}$. n sample: $P_{\rm laser} = 0.8\ \mu$W, $n_{\rm int} = 7 \times 10^{12}\ {\rm cm^{-3}}$. p sample: $P_{\rm laser} = 1.6\ \mu$W, $n_{\rm int} = 5 \times 10^{11}\ {\rm cm^{-3}}$.

[18] B. Huang and I. Appelbaum, Phys. Rev. B **82**, 241202 (2010).